Shock geometry and inverse Compton emission from the wind of a binary pulsar

Lewis Ball Jennifer Dodd

To appear in **Publ. Astronomical Soc. Aust.** 18/1
Submitted 19 Jul. 2000; Revised 8 Nov. 2000; Accepted 13 Nov. 2000

Research Centre for Theoretical Astrophysics, University of Sydney, N.S.W. 2006, Australia
ball@physics.usyd.edu.au

Abstract

PSR B1259−63 is a 47ms radio pulsar with a high spin-down luminosity which is in a close, highly eccentric 3.5-year orbit about a bright stellar companion. The binary system may be a detectable source of hard γ-rays produced by inverse Compton scattering of photons from the B2e star SS2883 by electrons and positrons in the pulsar wind. The star provides an enormous density of optical photons in the vicinity of the pulsar, particularly at epochs near periastron. We calculate the emission from the unshocked region of the pulsar wind, assuming that it terminates at a shock where it attains pressure balance with the companion's wind. The spectra and light curves for the inverse Compton emission from the shock-terminated wind are compared with those for an unterminated wind. If the pulsar's wind is weaker than that from the companion star, the termination of the wind decreases the inverse Compton flux, particularly near periastron. The termination shock geometry has the effect of decreasing the asymmetry of the γ-ray light curve around periastron, which arises because of the asymmetrical variation of the scattering angle.

Keywords: Pulsars; Inverse Compton scattering; Gamma-rays; Cherenkov telescopes; Pulsars: individual (PSR B1259−63)

1 Introduction

PSR B1259−63 is one of only three known radio pulsars which have a main sequence star binary companion. Such systems provide a unique environment for inverse Compton scattering because of the presence of an enormous density of low energy (optical) photons which serve as targets for electrons and positrons in the pulsar wind. The modest spin-down luminosity, and relatively high distance to two of these systems together imply that they are unlikely to be detectable sources of inverse Compton emission. In contrast, PSR B1259−63 is a galactic radio pulsar with a high spin-down luminosity ($L_{\rm p} = 8.3 \times 10^{28}$ W) and is relatively nearby (1.5 kpc). If just 0.1% of the wind luminosity is scattered into hard γ-ray photons the resulting flux should be detectable using current γ-ray telescopes.

PSR B1259−63 is in a highly eccentric orbit ($e \sim 0.87$) around SS2883, a B2e star of radius $R_* \sim 6R_\odot$ and luminosity $L_* \sim 8.8 \times 10^3\, L_\odot$ [Johnston et al. 1992, 1994, 1996]. At periastron the

Be-star photons at the pulsar, corresponding to an energy density of $U_{\rm rad} \sim 6 \times 10^{11}\,{\rm eV\,cm^{-3}}$. This is some 11 orders of magnitude larger than the typical background target density available for inverse Compton scattering by the winds of isolated pulsars.

The Crab is presently the only pulsar for which observations place any constraints on the physical parameters of a pulsar wind. Observations of the PSR B1259−63 system aimed at detecting hard γ-ray inverse Compton emission are planned during 2000. If successful they should provide the first direct probe of the freely-expanding region of the wind of any rotation-powered pulsar, and serve to constrain wind models and parameters.

In the absence of an efficient deceleration process the relativistic wind of a pulsar will expand freely until it attains pressure balance with the surrounding medium. If the wind is still supersonic at the point of pressure balance it will be bounded by a termination shock. Kirk, Ball & Skjæraasen [1999] investigated the γ-ray emission from PSR B1259−63 resulting from inverse Compton scattering by the shocked pulsar wind, downstream of the termination shock, where the pulsar wind electrons and positrons have been accelerated and isotropised as the radial flow of the wind is disrupted. The effects of the cooling of the shocked wind by inverse Compton scattering were included by Tavani & Arons [1997] in their model for the synchrotron emission from the system. Ball & Kirk [2000a] considered the effects of inverse Compton scattering by the unshocked pulsar wind, upstream of the termination shock. They calculated the deceleration of the wind that occurs as a result of 'inverse Compton drag' as energy and momentum are transferred from the wind to the scattered photons. In particular it was shown that the inverse Compton losses were unlikely to contain the wind of PSR B1259−63 before it attains the radius at which pressure balance with the Be-star outflow is likely to occur. Ball & Kirk [2000a] then calculated the emission from the freely-expanding wind subject to the assumption that the wind was not terminated by pressure balance.

In this paper we recalculate the inverse Compton emission from the unshocked wind of PSR B1259−63 including the effects of termination of the radially-expanding pulsar wind as a result of pressure balance with the Be-star wind. The relative strengths of the pulsar and Be-star winds are unknown. If the Be-star wind dominates then the termination shock will be close to, and wrapped around, the pulsar. This will have the effect of decreasing the emission from the unshocked portion of the wind, and the effects vary over the binary orbit of the system. We hope that inverse Compton γ-rays will be detected from PSR B1259−63 in the near future, providing data that can be compared with such models.

The calculation of the geometry of the termination shock is outlined in §2. In §3 we present γ-ray spectra and light curves from the terminated wind, and compare them with those calculated for the unterminated wind by Ball & Kirk [2000a]. Our conclusions are presented in §4.

2 Shock geometry

The winds of the pulsar and its companion star will generally be separated by a pair of termination shocks separated by a contact discontinuity. The shock structures enclose the star with the weaker wind. Giuliani [1982] developed a general description of axisymmetric flows that can be applied to the interaction of two such winds. Girard & Willson [1987; hereafter GW87] followed this description and derived the equations that describe the shape and position of the boundary separating two stellar winds subject to the following assumptions:

1. The shape of the shock is not affected by the orbital motion of the two stars. This implies azimuthal symmetry about the line joining the two stars.

3. Both winds are emitted radially with no angular dependence.
4. The winds are non-relativistic.

The resulting set of three ordinary differential equations (ODEs) can be integrated directly to find the position of the boundary, which can be loosely referred to as the 'shock', given the assumption of negligible thickness. The winds are characterised by their mass loss rate $\dot{M}$ and (constant) radial velocity u and these enter the equations that describe the shock geometry only in terms of the ratios

$$m = \frac{\dot{M}_1}{\dot{M}_2} \qquad \text{and} \qquad w = \frac{u_1}{u_2} \tag{1}$$

where the subscripts refer to the different stars. GW87 argued that the results obtained depended only on the quantity $\eta = mw$, although m and w enter the ODEs separately. In an alternative formulation presented by Huang & Weigert [1982] the quantities m and w only enter the ODEs as their product η.

Assumption (4) listed above is almost certainly not valid for a pulsar wind, which is likely to be highly relativistic. Modelling of the nebula produced by the wind of the Crab pulsar implies that the wind has a bulk Lorentz factor of $\gamma \sim 10^6$ at radii well beyond the light cylinder [Kennel & Coroniti 1984]. Melatos, Johnston & Melrose [1995] considered the interaction of a relativistic wind of PSR B1259−63 comprised primarily of electrons and positrons, with a wind from SS2883 dominated by much more massive ions. They showed that when the ions are dominant in both number and energy density, as is expected in PSR B1259−63/SS2883, the dependence of the geometry only on the product of m and w is lost. Nevertheless, for a given value of η the opening angles calculated by Melatos, Johnston & Melrose [1995] are within a factor of ~ 2 of the results of GW87 for a wide range of values of w/m.

In the following we approximate the shock position in the PSR B1259−63/SS2883 system using the formulation of GW87. This minimises the number of poorly known wind parameters that affect the results. The shock position is represented by its radial distance from the pulsar $r_{\rm T}(\alpha)$ where α is the angle between the lines joining the pulsar to the shock and the pulsar to the Be star.

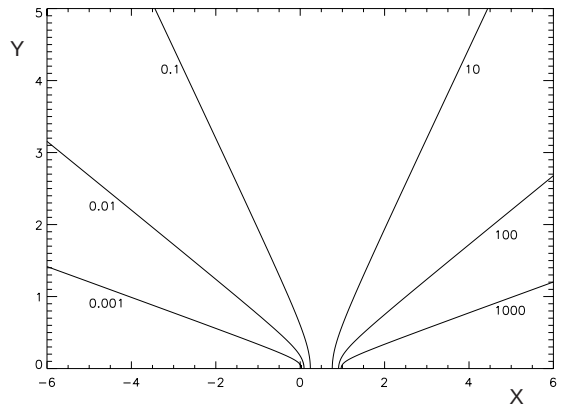

Figure 1: Shock positions calculated from the formulation of GW87. The pulsar is at (0,0) and the Be star is at (1,0). The values of η are as labelled.

the ODEs of GW87 for six different values of η. The quantity η is the ratio of the rates at which the stars are transferring momentum to their winds. When star 1 is taken to be the pulsar and star 2 is the Be star it follows that

$$\eta = \frac{L_p/c}{\dot{M}v} \tag{2}$$

where $\dot{M}$ and v are the mass loss rate and speed of the Be-star wind, and $L_{\rm p}$ is the spin-down luminosity of the pulsar. When $\eta < 1$ the Be-star wind dominates the pulsar wind, and the TS wraps around the pulsar. As η increases the apex of the TS moves further from the pulsar, the opening angle increases, and for $\eta > 1$ the pulsar wind is dominant and the TS wraps around the Be star.

The standoff distance from the pulsar to the apex of the TS is

$$r_{\rm T}(0) = \frac{\sqrt{\eta}}{1+\sqrt{\eta}}\, D \tag{3}$$

where D is the stellar separation. At large distances from the stars the momenta of the winds are almost parallel and the shock tends asymptotically to a cone characterised by a half-opening angle ψ and distance to the apex $\rho_{\rm c}$. A useful empirical approximation for ψ as a function of η is [Eichler & Usov 1993]:

$$\psi = 2.1 \left(1 - \frac{\bar{\eta}^{\frac{2}{5}}}{4}\right) \bar{\eta}^{\frac{1}{3}} \tag{4}$$

where $\bar{\eta} = \min(\eta, \eta^{-1})$. Figure 2 shows the geometry of the termination shock and illustrates the parameters used to describe it. We use θ to denote the value of α corresponding to the line of sight from Earth to the pulsar; i.e. θ is the angle between the line of sight and the line from the pulsar to the Be star.

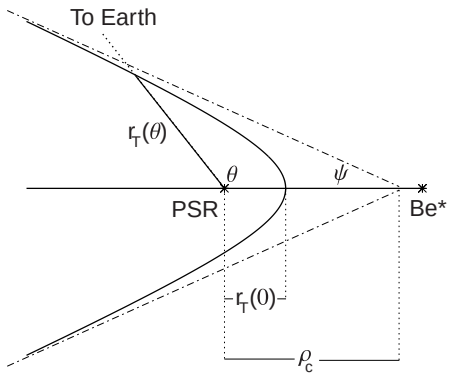

Figure 2: Geometry of the termination shock.

The Be star companion of PSR B1259−63 possesses an excretion disk which the pulsar passes through near periastron [Johnston et al. 1996, 1999; Ball et al. 1999]. This disk will dominate the termination of the pulsar wind for 50 days or so near periastron, greatly complicating the physics of the pulsar wind system at these epochs. Its effects on unpulsed X-ray emission close to periastron have been considered by Tavani & Arons [1997]. However its presence is irrelevant for the majority of the 1237 day binary orbit and it is neglected here. The results presented below can therefore not be taken to be accurate at epochs close to periastron.

Ball & Kirk [2000a; Equation 15] derived an expression for the radiation transfer that determines the intensity of the radiation emitted at the normalised energy $\epsilon_{\rm out} = E_{\rm out}/m_{\rm e}c^2$. Furthermore, it was shown that absorption of the scattered photons due to pair production on the Be-star photons is negligible. It follows that when the termination of the wind is included, the scattered intensity can be written as a line of sight integral of the scattering due to electrons moving radially out from the pulsar,

$$I(\epsilon_{\rm out}) = \int_0^{r_{\rm T}(\theta)} \left(\frac{L_{\rm p}}{4\pi}\right) \frac{\epsilon_{\rm out}}{\gamma_{\rm w}(0) m_{\rm e} c^3} \frac{{\rm d}N_\gamma}{{\rm d}\epsilon_{\rm out}{\rm d}t} \, {\rm d}s \ , \tag{5}$$

where the fraction of the wind momentum carried by ions is assumed to be negligible. The quantity $\gamma_{\rm w}(0)$ is the initial Lorentz factor of the pulsar wind and ${\rm d}N_\gamma/{\rm d}\epsilon_{\rm out}{\rm d}t$ is the differential rate of emission of inverse Compton scattered photons by a single electron. In the calculations of Ball & Kirk [2000a] the TS was assumed to be very distant from the pulsar, so that the upper limit of the integration was effectively infinity.

The termination of the pulsar wind will necessarily have the largest effect on its inverse Compton emission for small values of θ, since regardless of the value of η, $r_{\rm T}(\alpha)$ is a monotonically increasing function. Furthermore, these effects will be most significant if η is small, since in such cases the pulsar wind terminates close to the pulsar. The orbit of the PSR B1259−63 system is inclined at $i = 35^\circ$ to the plane of the sky, so an observer samples angles θ between $90 - i = 55^\circ$ and $90 + i = 125^\circ$ over the binary period. The variation of θ over the orbit is shown in Figure 3. If $\eta \ll 1$ the pulsar wind will terminate very close to the pulsar for small θ, decreasing the observable emission from the unshocked wind most significantly at binary phases which correspond to values of θ that are close to the minimum, i.e. between around day −200 and periastron.

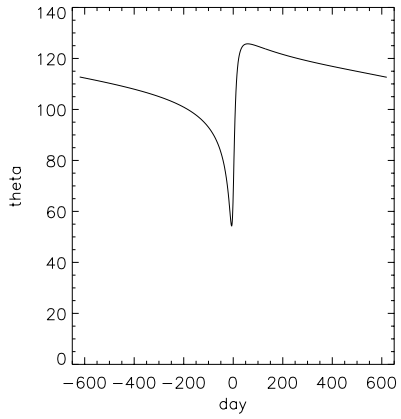

Figure 3: The variation of the angle θ between the line of sight to PSR B1259−63 and the line joining the pulsar and its Be-star companion over the binary orbit. Day 0 corresponds to periastron, which next occurs on 2000 October 17.

3.1 Spectra

Figure 4 shows the spectra of inverse Compton emission for two values of η for which the Be-star wind dominates the pulsar wind, which therefore terminates quite close to the pulsar for small θ. The quantity plotted is the spectral energy distribution EF_E where F_E is the energy flux at

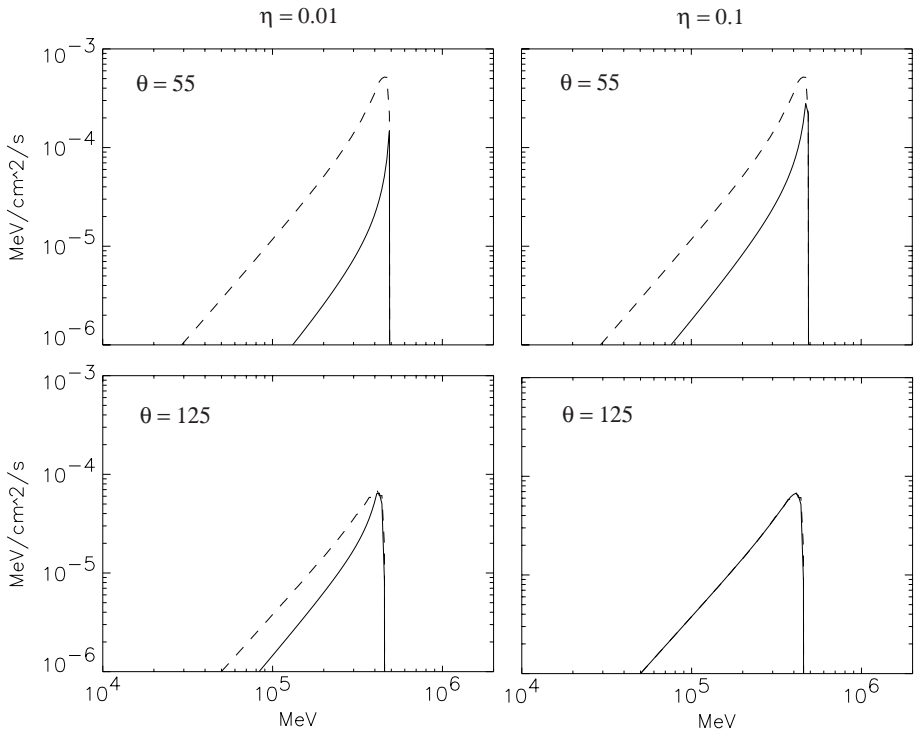

Figure 4: Inverse Compton emission spectra for the unterminated (dashed lines) and terminated (solid lines) pulsar wind, for $\eta = 0.01$ (left panels) and $\eta = 0.1$ (right panels). The top row shows the spectra for $\theta = 55°$, and the bottom row is for $\theta = 125°$, the extremes of this angle that can be sampled from Earth. All the spectra shown have been calculated for a pulsar wind with an initial Lorentz factor $\gamma_{\rm w}(0) = 10^6$.

Earth of inverse Compton scattered photons of energy E. The solid lines show the results when the termination of the pulsar wind is included, and the dashed lines show the spectra calculated by Ball & Kirk [2000a] when the shock termination is very distant from the pulsar. The spectra are shown assuming that the separation of the pulsar and the Be star is that which applies at periastron, and have been calculated for the extreme values of θ that can be sampled from Earth. Both of these extreme values occur very close to periastron, as can be seen from Figure 3, so the assumption of periastron separation is appropriate. Furthermore, it is assumed that the spectrum of target photons from the Be star can be approximated as a monochromatic distribution at a normalised energy $\epsilon_0 = 2.7 k_{\rm B} T_{\rm eff}/(mc^2) \approx 10^{-5}$ where $T_{\rm eff}$ is the star's effective temperature. Calculations including a more realistic Be-star spectrum have been presented by Ball & Kirk [2000b] and Kirk, Ball & Skjæraasen [2000]. The effects of including a better approximation to the target photon spectrum are generally small, but may warrant closer investigation if the system is detected in hard γ-rays.

All the spectra in Figure 4 are sharply peaked at an energy close to 5×10^5 MeV, somewhat lower than the Thomson limit of $\gamma_{\rm w}(0)^2 m_{\rm e} c^2 \epsilon_0 \approx 5 \times 10^6$ MeV because of the importance of Klein–Nishina effects. In the Klein–Nishina regime, i.e. when $\gamma\epsilon_0 \gtrsim 1$, a scattering particle loses a significant fraction of its energy to the scattered photon and the maximum scattered energy is then $\epsilon_{\rm out}^+ \sim \gamma$. The upper limit of the emission spectrum is unaffected by the inclusion of the TS, since the scatterings that produce photons of this energy involve undecelerated electrons (with

from the pulsar the wind electrons lose energy via the inverse Compton scattering process. Lower energy scattered photons are generated farther from the pulsar, and so tend to be suppressed by the termination of the wind.

For small θ and small η the TS is very close to the pulsar where inverse Compton scattering is still very efficient because the target photon density is large and the scatterings are close to head on. The wind is terminated before it has been decelerated to Lorentz factors significantly below $\gamma_{\rm w}(0)$, so the scattering electrons are essentially monochromatic, as are the target photons in our approximation. This has the effect of dramatically reducing the emission at all energies below the upper cutoff, producing a scattered spectrum that is even more sharply peaked than that resulting from the unterminated wind. Such a case is illustrated in the top left panel for $\eta = 0.01$ and $\theta = 55^\circ$, for which the scattered spectrum is essentially monochromatic at the upper cutoff.

The TS radius increases rapidly with increasing α (for a given η), with the rate of increase approaching infinity as α approaches $180^\circ - \psi$ where ψ is the half-opening angle of the cone and $\eta < 1$ is assumed. At energies near the upper cutoff the scattered spectrum from the terminated wind therefore rapidly approaches that from the unterminated wind as θ increases. The suppression at lower energies, which are produced by scatterings well away from the pulsar where the wind has been significantly decelerated, persists to larger θ. This effect is dramatically illustrated by a comparison between each top panel of Figure 4 with the corresponding lower panel. For the case where $\theta = 125^\circ$ and $\eta = 0.01$ the emission at and just below the cutoff energy is essentially unaffected by the inclusion of the TS, because the scatterings that produce photons of these energies occur closer to the pulsar than does the TS.

For larger values of η the TS occurs further from the pulsar. It follows that for a given θ, the difference between the inverse Compton emission from the terminated and the unterminated wind decreases as η increases. For the case shown in the lower right panel of Figure 4, with $\eta = 0.1$ and $\theta = 125^\circ$, the TS occurs so far from the pulsar that it has essentially no effect on the scattered emission in the energy range shown, though it does reduce the scattered flux at even lower energies.

3.2 Light curves

For $\eta > 1$ the TS wraps around the Be star and the line of sight to the pulsar does not intersect the shock if $\theta > \psi$. Equation (4) implies that for $\eta \gtrsim 7$, $\psi \lesssim 55^\circ$ which is the minimum observable value of θ over the binary orbit of PSR B1259−63. Thus if $\eta \gtrsim 7$ the line of sight doesn't intersect the TS at any phase of the binary orbit, the TS has no effect on the observable inverse Compton emission from the freely-expanding wind, and the results of Ball & Kirk [2000a] require no modification.

For $\eta < 1$ the TS wraps around the pulsar and is intersected by the line of sight to the pulsar if $\theta < 180^\circ - \psi$. It follows from Equation (4) that if $\eta \lesssim 0.14$, $180^\circ - \psi \gtrsim 125^\circ$ which is the maximum observable value of θ, and thus the line of sight to the pulsar intersects the TS at all binary phases.

Figure 5 shows the orbital variation of the integrated flux density $\int F_E \, {\rm d}E$, expected from PSR B1259−63 for $\gamma_{\rm w}(0) = 10^6$. The dashed curve shows the emission from the unterminated wind as calculated by Ball & Kirk [2000a]. The solid line shows the emission when the wind is terminated by a shock at the position shown in Figure 1 for $\eta = 0.1$. The TS is wrapped around the pulsar and is intersected by the line of sight to the pulsar at all binary phases. However, between days +50 and +400 the intersection point is sufficiently distant from the pulsar that it is beyond those radii where the majority of the inverse Compton scattering occurs. The termination of the wind therefore has little effect in reducing the inverse Compton emission in this period, and

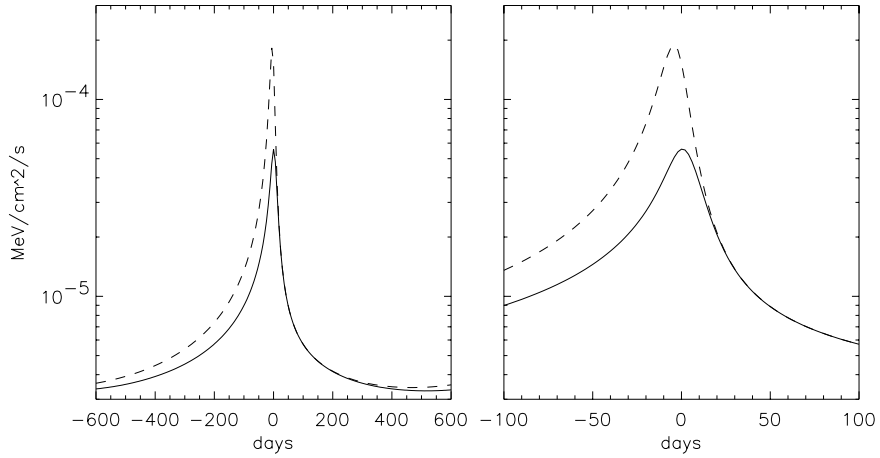

Figure 5: Light curves showing the integrated energy flux at the Earth from PSR B1259−63 over the whole orbital period (left panel), and over 200 days centred on periastron (right panel). The initial Lorentz factor of the pulsar wind is $\gamma_{\rm w}(0) = 10^6$. The dashed curves show the emission from an unterminated wind as calculated by Ball & Kirk [2000a]. The solid curves show the emission when the wind is terminated by a shock whose position is determined by the parameter $\eta = 0.1$.

the light curve from the terminated wind is indistinguishable from that of an unconfined wind.

The effect of the termination of the wind is asymmetric because of the asymmetry in the dependence of the line-of-sight angle θ about periastron. The angle θ decreases very rapidly towards its minimum value just prior to periastron, which implies that the radius at which the line of sight to the pulsar intersects the TS does the same. The increase from the minimum value of θ to the maximum then occurs very rapidly, starting just a few days before periastron. The termination of the wind therefore decreases the emission from the freely expanding portion of the pulsar wind most effectively prior to periastron, and thus has the effect of decreasing the characteristic asymmetry in the γ-ray light curve about periastron. For $\eta = 0.1$ Figure 5 shows that the effect of the TS is to reduce the maximum integrated inverse Compton flux density by a factor of ~ 4, to make the time at which the maximum occurs a few days later, and to reduce the asymmetry about periastron measured by the ratio of the integrated fluxes at days ± 50, from ~ 3 to ~ 1.6.

Figure 6 shows the light curve for a shock-terminated wind with $\eta = 0.01$. In this case the shock is so tightly wrapped around the pulsar that its intersection with the line of sight to the pulsar always occurs at a radius where inverse Compton scattering is still effective. The emission from the terminated wind is thus substantially less than that from an unconfined wind throughout the binary orbit. The observable flux in this case is reduced by a factor of between 1.5 and 3 over roughly 80% of the orbital period. The maximum integrated hard γ-ray flux density is a factor of ~ 10 lower than that from an unterminated wind and occurs ~ 6 days later, and the ± 50 day asymmetry is actually reversed to ~ 0.95.

4 Discussion and conclusions

Ball & Kirk [2000a] argued that inverse Compton emission from the freely-expanding portion of the wind of PSR B1259−63 should be detectable at energies somewhere between GeV and TeV, depending on the wind parameters. The results presented in Section 3 suggest that even if the

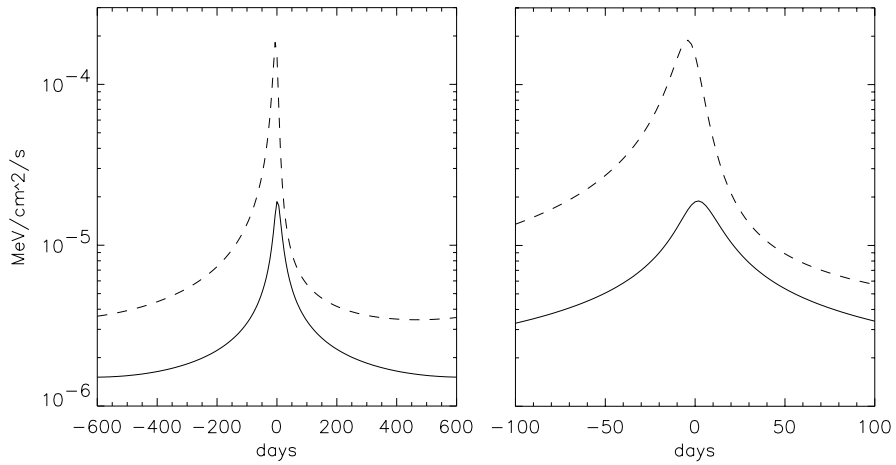

Figure 6: Light curves showing the integrated energy flux at the Earth from PSR B1259−63 when the wind is terminated by a shock whose position is determined by the parameter $\eta = 0.01$ (solid curve). The initial Lorentz factor of the wind is $\gamma_{\rm w}(0) = 10^6$. The dashed curves show the emission from an unterminated wind as calculated by Ball & Kirk [2000a] (and are identical to those in Figure 5).

wind of the Be star dominates that of the pulsar, terminating it in a shock which wraps around the pulsar, the scattered emission should still be detectable for a wide range of wind parameters. However, the TS has the effect of decreasing the peak integrated γ-ray flux from the freely-expanding wind, and of decreasing the asymmetry which otherwise produces a characteristic light curve which shows a higher γ-ray flux before periastron than after.

Even if the Be-star wind dominates to such a degree that the unshocked pulsar wind is not detectable, the models of Kirk, Ball & Skjæraasen [1999] indicate that inverse Compton emission from the shocked pulsar wind should be above the thresholds of current detectors.

The scattered γ-ray signal from this system is most likely to comprise a combination of emission from the shocked and unshocked regions of the pulsar wind. The reduced asymmetry and periastron to apastron ratio of the emission from the terminated wind may make it harder to deconvolve the two contributions, but only detailed modelling of real data will provide such answers.

The best opportunity for detecting such emission in the near future is afforded by the new CANGAROO II imaging Cherenkov telescope located in Australia [Yoshikoshi et al. 1999]. When the present lack of operational γ-ray telescopes is relieved by the launch of the GLAST and INTEGRAL observatories, inverse Compton emission from this pulsar system may well be detectable at lower energies in the MeV–GeV range.

The next periastron of PSR B1259−63 occurs in October 2000. CANGAROO II observations of the system will not be possible at times near periastron because at that time the object will be too close to the Sun. In any event, the light curves shown in Figures 5 and 6 are not realistic between about days −25 and +25 because we have not modelled the interaction with the Be-star disk which is important at such epochs. Observations of the PSR B1259−63 system with CANGAROO II are planned for July and December 2000, when our models of the inverse Compton emission from the system should be applicable. If such observations are successful in detecting hard γ-ray emission from this unique pulsar system they should provide valuable insights into the properties of the pulsar wind. In particular, detection of inverse Compton γ-ray emission from the system should help to constrain values of the bulk Lorentz factor of the pulsar wind and the

References

Ball, L., & Kirk, J. G., 2000a, Astropart. Phys., 12, 335
Ball, L., & Kirk, J. G., 2000b, ASP Conf., 202, 531
Ball, L., Melatos, A. M., Johnston, S., Skjæraasen, O., 1999, ApJ, 541, L39
Eichler, D., Usov, V., 1993, ApJ, 402, 271
Girard, T., Willson, L. A., 1987, A& A, 183, 247
Giuliani, J. L., 1982, ApJ, 256, 634
Huang, R. Q., Weigert, A., 1982, A&A, 112, 281
Johnston, S., Manchester, R. N., Lyne, A. G., Bailes, M., Kaspi, V. M., Qiao, G., D'Amico, N., 1992, ApJ, 387, L37
Johnston, S., Manchester, R. N., Lyne, A. G., Nicastro, L., Spyromilio, J., 1994, MNRAS, 268, 430
Johnston, S., Manchester, R. N., Lyne, A. G., D'Amico, N., Bailes, M., Gaensler, B. M., Nicastro, L., 1996, MNRAS, 279, 1026
Johnston, S., Manchester, R. N., McConnell, D., Campbell-Wilson, D., 1999, MNRAS, 302, 277
Kennel, C. F., Coroniti, F. V., 1984, ApJ, 283, 710
Kirk, J. G., Ball, L., Skjæraasen, O., 1999, Astropart. Phys., 10, 31
Kirk, J. G., Ball, L., Skjæraasen, O., 2000, ASP Conf., 202, 527
Melatos, A., Johnston, S., Melrose, D. B., 1995, MNRAS, 285, 381
Tavani, M., Arons, J., 1997, ApJ, 477, 439
Yoshikoshi, T., et al., 1999, Astroparticle Phys., 11, 267